

<https://doi.org/10.1038/s41612-024-00737-8>

Global latitudinal patterns in forest ecosystem nitrous oxide emissions are related to hydroclimate

Check for updates

Jiayuan Liao^{1,2,3}, Wei Zheng², Qiong Liao^{4,5} & Sheng Lu^{1,4} ✉

Nitrous oxide (N₂O) emissions are a serious global issue, with substantial evidence indicating that hydroclimate processes significantly contribute to these emissions. Forests, covering one-third of global land, are key in the water cycle and influence hydroclimate processes, which vary with climate, latitude, and forest types. The role of hydroclimate in regulating global forest N₂O emission remains largely unknown. Our global analysis shows that hydroclimate factors dominate the latitudinal gradient of forest N₂O fluxes, which decrease with latitude. N₂O fluxes are highest in tropical forests, followed by temperate and boreal forests. Hydroclimate factors contribute 78.2% to N₂O fluxes, while soil factors contribute 21.8%. Our results urgently call for future studies to investigate the relationship between N₂O flux and hydroclimate factors like radiation, evapotranspiration, and vapor pressure deficits. Collectively, these findings highlight hydroclimate significant impact on N₂O emissions and suggest incorporating these factors into predictive models for greater accuracy.

Biogeochemical cycles are impacted by changes in land use cover^{1–3}. One of the primary issues in climate change assessment is determining how the nitrogen (N) cycle responds to changes in land cover^{4,5}. The world's forests cover tropical, temperate, and boreal zones, covering 4.06 billion hectares (ha), around 31% of the world's area^{6,7}. To date, studies on the biogeochemical effects of forests have mainly focused on changes in carbon (C) sinks and alteration in atmospheric CO₂ concentrations through changes in forest cover^{8–12}. However, compared to the forest C cycle, the forest N cycle has received little attention, particularly on a global scale.

Nitrous oxide (N₂O), a greenhouse gas produced during the N cycle, can significantly contribute to global warming and stratospheric ozone layer depletion¹³. Agriculture is the largest anthropogenic source of N₂O due to N fertilizer application, about 60% of all anthropogenic emissions, generating 4.1 Tg N/year¹⁴. As a result, much N₂O emissions research has concentrated on agricultural areas, leaving a gap in data from other types of land use, particularly forest ecosystems^{15,16}. Given that anthropogenic N emissions have enhanced N deposition in forest areas, forest N₂O emissions are expected to rise continuously in the future¹⁷. Thus, even though both soil N availability and N₂O emissions from forests are significantly lower than agriculture, the former is still a large source of N₂O on a global scale due to

their large area^{18–20}. Global scale in-depth research of forest N₂O emissions is crucial for future climate change estimates and the creation of effective greenhouse gas-reduction policies.

Previous studies showed that the biogeochemical N cycle is strongly influenced by hydroclimate processes^{21–25}. The two primary processes that control soil N₂O emissions in the N cycle, nitrification, and denitrification, are influenced by many environmental conditions^{26–28}. Studies have shown that nitrifiers and denitrifiers respond sensitively to hydroclimate factors, such as changes in soil moisture (SM) and temperature, which regulate their metabolic activities and gene abundance^{29–31}. Forests maintain the hydrological cycle via biophysical mechanisms that have been widely investigated and demonstrate a change in latitude from tropical to boreal areas^{6,32}. Global hydrologic patterns may affect the N cycle and thus global N₂O emissions^{16,33}. However, no studies have systematically coupled the N cycle and hydroclimate, identified the key driving variables, and related them to worldwide forest N₂O emissions³⁴. Such information would be relevant for management and decision-making but is still lacking.

To address this gap, here we report a systematic study, using in situ field observations and multi-source remotely sensed and gridded datasets to quantify assess the impact of hydroclimate on forests (tropical to boreal

¹Key Laboratory of Soil and Water Conservation and Desertification Combating in Hunan Province, College of Forestry, Central South University of Forestry and Technology, Changsha, Hunan, China. ²School of Atmospheric Sciences, Sun Yat-sen University, and Southern Marine Science and Engineering Guangdong Laboratory (Zhuhai), Zhuhai, Guangdong, China. ³Environmental Sciences and Engineering, Biological and Environmental Science and Engineering Division, King Abdullah University of Science and Technology, Thuwal, Kingdom of Saudi Arabia. ⁴Key Laboratory of Cultivation and Protection for Non-Wood Forest Trees of National Ministry of Education, College of Forestry, Central South University of Forestry and Technology, Changsha, Hunan, China. ⁵School of Chemical and Environmental Engineering, Hunan Institute of Technology, Hengyang, Hunan, China. ✉e-mail: lusheng@csuft.edu.cn

Fig. 1 | Distribution of the 69 study sites. Study sites were classified into tropical forests (25°S–25°N, number of sites=22, number of observation samples=61), temperate forests (25°S–50°S and 25°N–50°N, number of sites = 28, number of observation samples = 178), and boreal (north of 50°N, number of sites = 19, number of observation samples = 33) forests, based on their latitude. The circular pie plot represents the percentage of different types of forest sites, with the color harmonized with the color of the points.

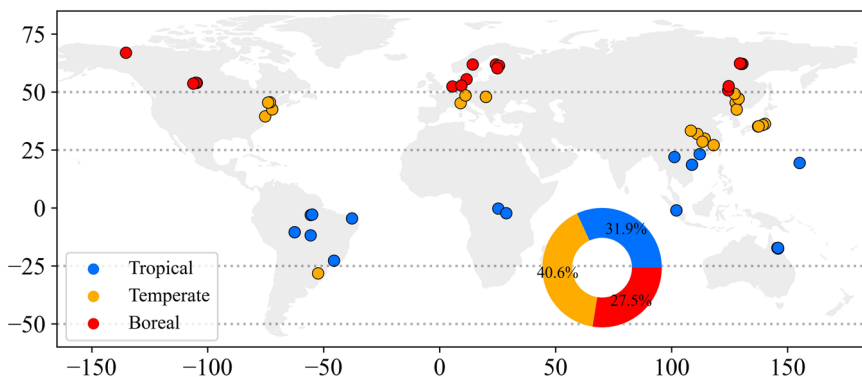
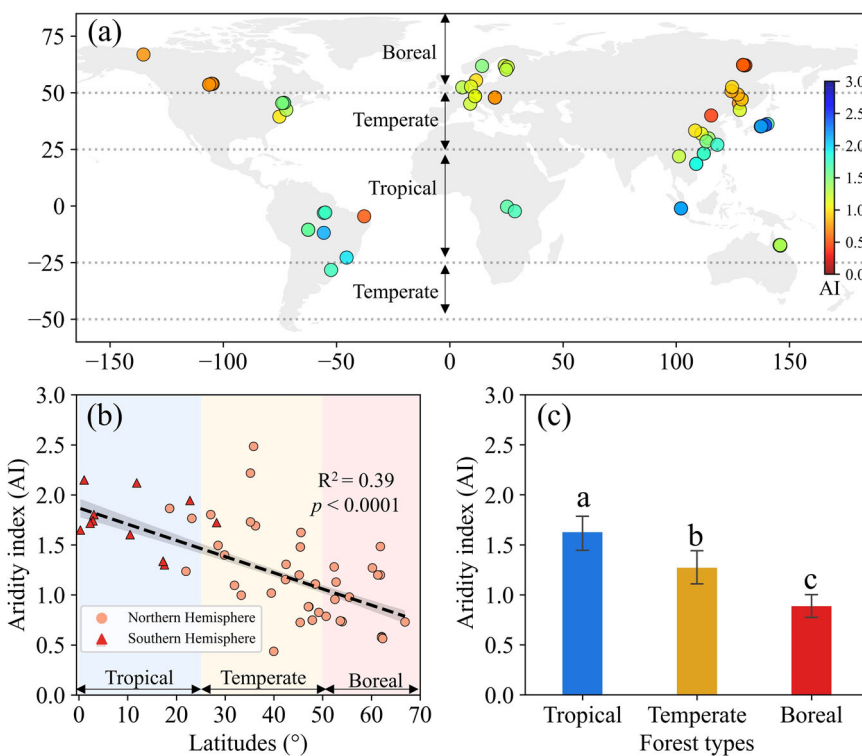


Fig. 2 | The climate of study sites. **a** Global patterns of aridity index (AI) across three forest types. The color bar represents the value of AI. **b** Relationship between latitudes and aridity index. R^2 and p values are shown in the figure when significant ($p < 0.05$). Regression lines (black lines), 95% confidence intervals (gray shading along the line). **c** Average value (mean \pm SD) of AI from tropical to boreal forest areas. Statistically significant differences among forests are represented by different lowercase letters ($p < 0.05$).



forests) N_2O emissions (Fig. 1). As the biophysical processes affecting the hydroclimate cycle have a distinct latitudinal pattern from the tropics to the boreal area^{6,32}. We aim to (a) investigate whether hydroclimate factors and N_2O emissions have a clear latitudinal gradient from the tropical to the boreal forest, and (b) determine the contribution of hydroclimate factors to the N_2O emission latitudinal gradient. Addressing these two questions will allow us to more accurately assess the impact of climate change on the land N cycle.

Results
Aridity index (AI) and N_2O fluxes from tropical to boreal forest areas

AI denotes the water balance between the land surface and the atmosphere, and its trend from tropical to boreal forest areas are given in Fig. 2a. AI decreases with latitudes ($R^2 = 0.39$, $p < 0.0001$, Fig. 2b), and the mean value (Fig. 2c) of tropical forest areas (1.6) is significantly higher than temperate forest areas (1.3) and boreal forest areas (0.9).

N_2O fluxes ($R^2 = 0.14$, $p < 0.0001$) and the cumulative ($R^2 = 0.28$, $p < 0.0001$) emissions significantly decreasing with latitudes (Figs. 3a, b and S1a). The value of N_2O fluxes in tropical forests, temperate forests, and boreal forests is 45.4 ± 97.4 , 37.7 ± 74.5 , and $11.6 \pm 24.1 \mu g \cdot m^{-2} \cdot h^{-1}$, respectively (Fig. 2b). The mean value of cumulative N_2O in tropical forests, temperate forests, and boreal forests is 2.5 ± 2.1 , 1.0 ± 1.1 , and $0.5 \pm 0.7 kg \cdot ha^{-1}$, respectively (Figure S1b).

N_2O flux emissions were highly positively correlated with cumulative emissions ($R^2 = 0.95$, $p < 0.0001$, Fig. S2), implying that the processes that drive N_2O fluxes and cumulative emissions are similar. As a result, in this work, we focus primarily on the results of N_2O flux emissions.

Variations in hydroclimate factors along latitude and forest types

We found a clear latitudinal gradient in all hydroclimate factors in this study (Fig. 4). Mean annual incoming shortwave radiation (R_{in} , $R^2 = 0.81$, $p < 0.0001$), mean annual temperature (MAT, $R^2 = 0.67$, $p < 0.0001$), mean

Fig. 3 | Forest N₂O fluxes emission globally. **a** Global patterns of N₂O fluxes. **b** Relationship between latitudes and N₂O fluxes. R² and p values are shown in the figure when significant (p < 0.05). Regression lines (black lines), 95% confidence intervals (gray shading along the line). Data of N₂O fluxes are logarithmically (LN) transformed before regression analysis. **c** Average value (mean ± SD) of N₂O fluxes from tropical to boreal forests. Statistically significant differences among forests are represented by different lowercase letters (p < 0.05).

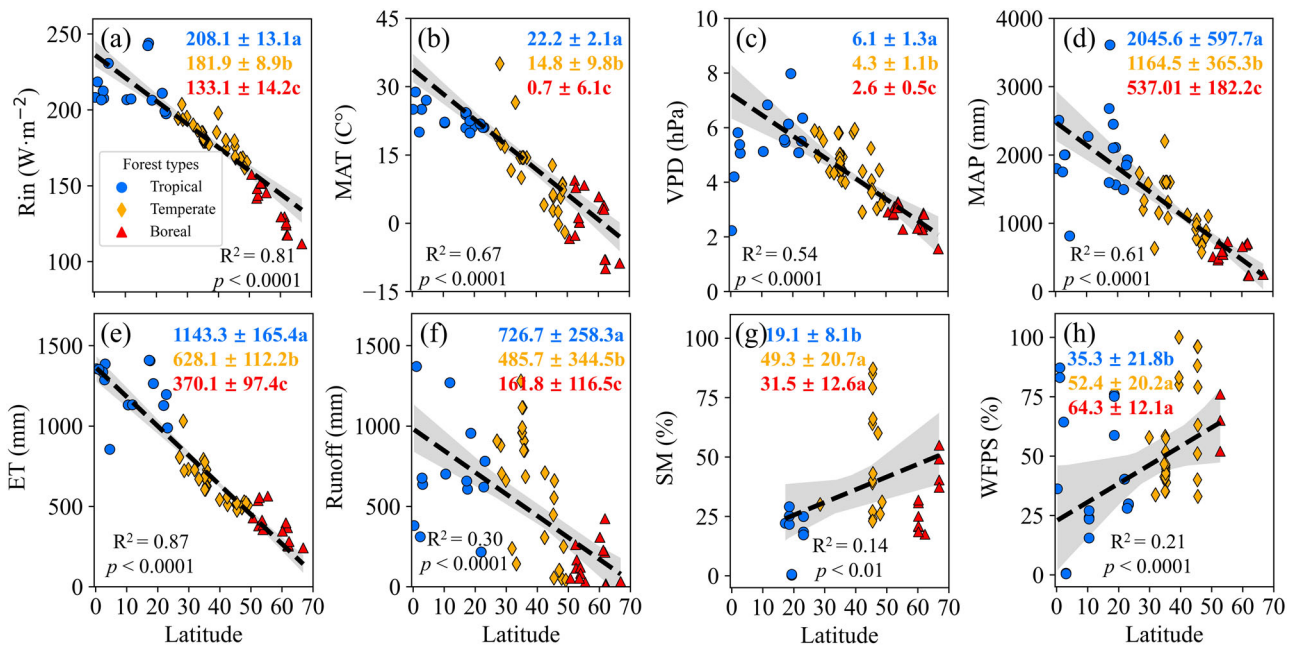
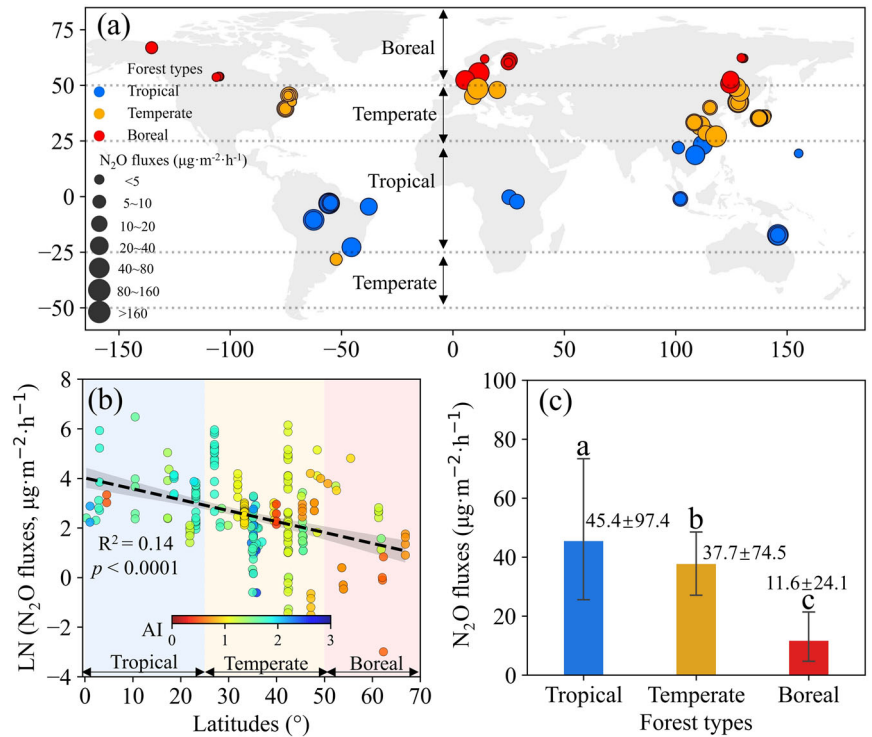


Fig. 4 | Variations in hydroclimate factors along latitude and forest types. **a** Rin (mean annual incoming solar radiation). **b** MAT (mean annual temperature). **c** VPD (mean annual vapor pressure deficits). **d** MAP (mean annual precipitation). **e** ET (actual annual evapotranspiration). **f** Runoff. **g** SM (soil moisture). **h** WFPS (water-filled pore space). R² and p values are shown in the figure when significant (p < 0.05). Regression lines (black lines), 95% confidence intervals (gray shading along the line). The average value (mean ± SD) of different variables of tropical (blue), temperate (orange), and boreal (red) forests are shown in each figure. Statistically significant differences among forests are represented by different lowercase letters (p < 0.05).

annual vapor pressure deficit (VPD, R² = 0.54, p < 0.0001), mean annual precipitation (MAP, R² = 0.61, p < 0.0001), actual annual evapotranspiration (ET, R² = 0.87, p < 0.0001), and Runoff (R² = 0.30, p < 0.0001) exhibit significantly negative relationships with latitudes (Fig. 4a–f). These factors varied significantly among forest types (p < 0.05), consistently showing tropical > temperate > boreal. SM (R² = 0.14, p < 0.01) and water-filled pore space

(WFPS, R² = 0.21, p < 0.0001) showed significantly positive relationships with latitudes (Fig. 4g, h). SM and WFPS are not statistically different in temperate and boreal forests (p > 0.05), while they are significantly greater in tropical forests (p < 0.05).

Interaction between hydroclimate factors is shown in Figs. S3–7. Solar radiation is crucial in determining land surface temperature and atmospheric

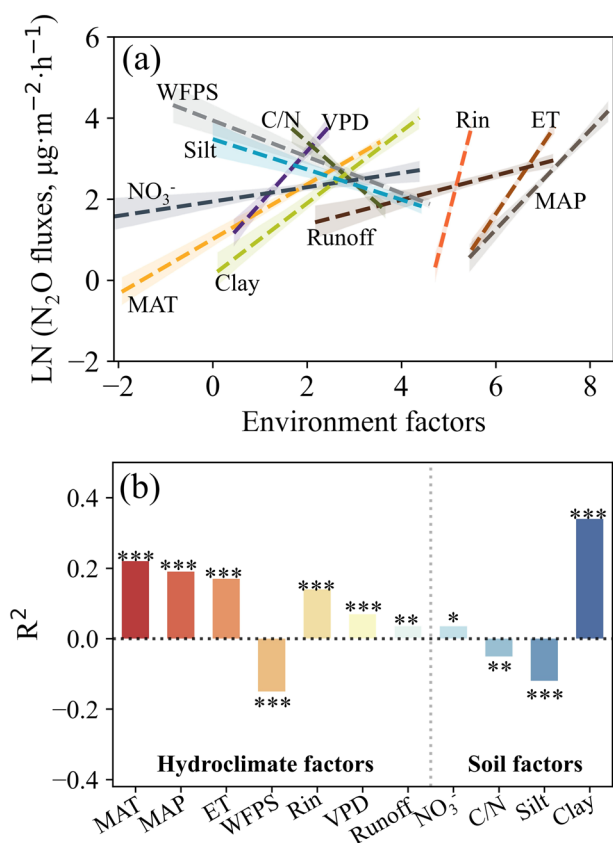


Fig. 5 | Correlation of environmental factors and N₂O flux emissions. **a** Linear regression analysis of environmental factors and N₂O flux emissions. Only the fitted lines with significant ($p < 0.05$) correlation are shown. Regression lines (dashed lines), 95% confidence intervals (shading along the line). Data are logarithmically transformed before regression analysis. **b** R^2 of linear regression analysis of each factor with N₂O flux emissions, less than 0 means negative correlation, and more than 0 means positive correlation. * $p < 0.05$; ** $p < 0.01$; *** $p < 0.001$.

moisture requirements, as MAT ($R^2 = 0.64$, $p < 0.0001$), VPD ($R^2 = 0.53$, $p < 0.0001$), and ET ($R^2 = 0.69$, $p < 0.0001$) are significantly increased with Rin (Fig. S3). Rin can affect ET directly and can also increase ET indirectly by affecting MAT and VPD (Fig. S4). ET significantly increased with MAT ($R^2 = 0.54$, $p < 0.0001$) and VPD ($R^2 = 0.41$, $p < 0.0001$) (Fig. S5). As ET increases, SM ($R^2 = 0.15$, $p < 0.01$) and WPFS ($R^2 = 0.16$, $p < 0.0001$) decrease significantly (Fig. S6). In addition, soil moisture was significantly influenced by runoff (Fig. S7). These results explain why soil moisture increases with latitudes since solar radiation, temperature, and VPD decrease with latitudes, lowering ET and thereby preserving more water in the soil.

Variations in soil physical and chemical properties along latitude and forest types

We also tested for soil factor's latitude pattern that might explain some of the variations in the magnitude of N₂O fluxes. (Figure S8 and S9). soil organic carbon content (SOC, $R^2 = 0.12$, $p < 0.0001$), total nitrogen content (TN, $R^2 = 0.077$, $p < 0.01$), ratio of SOC to TN (C/N, $R^2 = 0.032$, $p < 0.05$), nitrate nitrogen content (NO₃⁻, $R^2 = 0.12$, $p < 0.0001$), and silt content ($R^2 = 0.23$, $p < 0.0001$), exhibit significantly positive relationships with latitudes (Fig. S8a–e), while clay content ($R^2 = 0.25$, $p < 0.0001$), bulk density (BD, $R^2 = 0.11$, $p < 0.0001$), and altitude ($R^2 = 0.12$, $p < 0.05$) significantly negative correlation with latitudes (Fig. S8f–h). No significant ($p > 0.05$) correlation of soil ammonia nitrogen content (NH₄⁺), pH, and sand content with latitudes was observed (Fig. S9). Among these soil factors, only clay showed significant differences among the three forest types, with size classes showing tropical > temperate > boreal forests ($p < 0.05$, Fig. S8f).

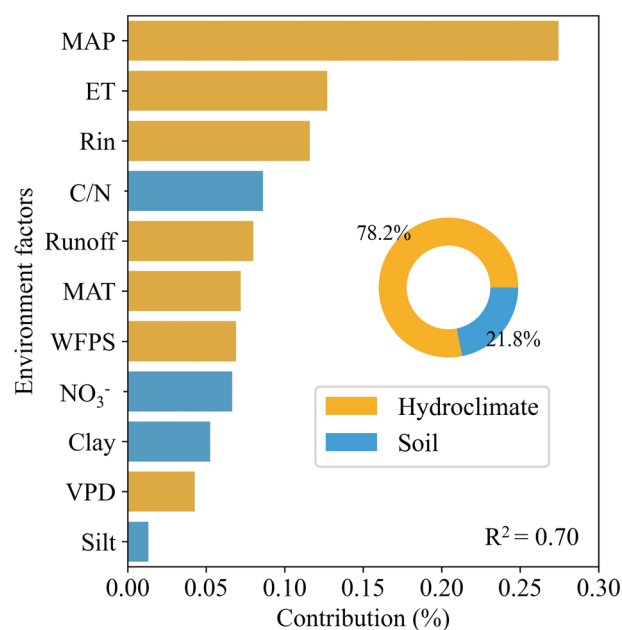


Fig. 6 | The relative influence of hydroclimate and soil factors on N₂O flux emissions. The importance values (contribution, %) are derived from a random forest analysis. Data are logarithmically transformed before analysis. Barplots and donut charts indicate the relative influence of different factors on N₂O flux emissions.

Relationships among environmental factors and N₂O fluxes

Further, we investigated the correlation of N₂O fluxes with different factors (those with significant latitudinal gradients in the above results). Linear regression analysis of hydroclimate factors and soil physicochemical properties on N₂O fluxes are shown in Fig. 5. Except for SM, all hydroclimate parameters have a significant correlation with N₂O fluxes, and only WPFS has a negative influence ($p < 0.05$). Of the 11 soil factors, only 4 were significantly correlated with N₂O fluxes. Soil NO₃⁻ and clay are positively related to N₂O fluxes ($p < 0.05$), while C/N and silt revealed opposite relationships with N₂O fluxes ($p < 0.05$). In this study, a total of 11 factors were significantly correlated with N₂O fluxes, of which 7 hydroclimate factors (accounted for 63.6%).

Relative contribution of environmental factors to N₂O fluxes

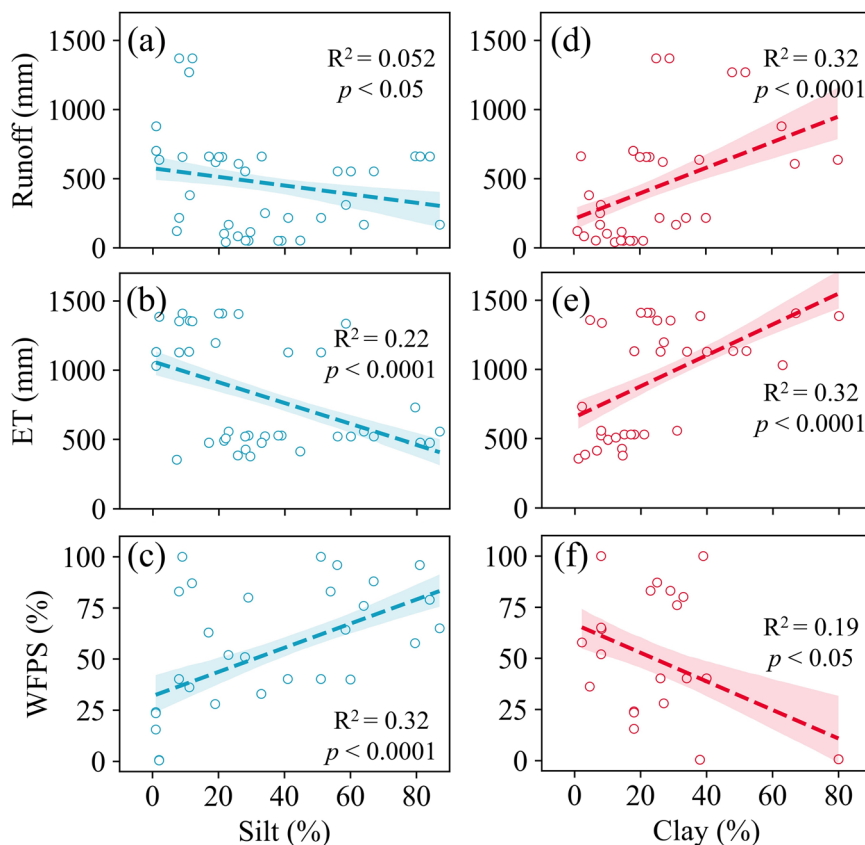
Finally, we used random forest to examine the relative contributions of the 11 parameters listed above to N₂O fluxes (Fig. 6). The random forest analysis found that the most crucial variable affecting N₂O fluxes was the hydroclimate factors (i.e., MAP, ET, Rin), followed by C/N. Among hydroclimate factors, the relative contribution rank of each factor was: MAP > ET > Rin > C/N > MAT > WPFS > VPD. For soil factors, the relative contribution rank of each factor was C/N > NO₃⁻ > clay > silt. Overall, random forest analysis indicated that the key factor that determined the N₂O flux was the hydroclimate, which cumulative contribution amounted to 78.2%.

Of four (C/N, NO₃⁻, clay, and silt) key soil factors, we found that soil texture (clay and silt) had a significant effect on water condition (runoff, ET, and WPFS, Fig. 7). Runoff and ET decreased with silt ($R^2 = 0.052$, $p < 0.05$; $R^2 = 0.22$, $p < 0.0001$, respectively, Fig. 7a, b), while increased with clay ($R^2 = 0.32$, $p < 0.0001$; $R^2 = 0.32$, $p < 0.0001$, respectively, Fig. 7d, e). WPFS is positively correlated with silt ($R^2 = 0.32$, $p < 0.0001$, Fig. 7c), and has a negative correlation with clay ($R^2 = 0.19$, $p < 0.05$, Fig. 7f).

Discussion

Many environmental factors influence N₂O emissions, resulting in exceptionally high temporal and spatial variability in fluxes^{28,30,35,36}. It is one of the main reasons for the persistent difficulties in suppressing N₂O fluxes^{37,38}. Previous studies have shown that patterns of hydroclimate may affect soil N dynamics, such as availability and flux emissions^{16,21–24}. Forests cover a large

Fig. 7 | Relationship between soil texture and water condition. Linear regression analysis of the effect of soil silt content on runoff (a), ET (b), and WFPS (c). Linear regression analysis of the effect of soil clay content on runoff (d), ET (e), and WFPS (f). R^2 and p values are shown in the figure when significant ($p < 0.05$). Regression lines (dashed lines), 95% confidence intervals (shading along the line).



area, and their N_2O emission cannot be ignored. In addition, forests' hydroclimate processes showed a latitudinal transition from tropical to boreal areas^{6,39}. However, the study of the impact of hydroclimate on N_2O emissions latitude gradient at the global scale is still largely unknown³⁴. Our study fills this gap, on a global scale we found that hydroclimate factors explained 78.2% of forest N_2O emission variations, which decreased from tropical to boreal forests. The four potential main mechanisms (Fig. 8) are as follows: First, the frequency of drought-rewetting decreases with latitude, resulting in a decrease in N_2O fluxes from tropical to boreal forests. A recent study found that high atmospheric demand in the tropics induces excessive evapotranspiration, which accelerates the drawdown of soil moisture, resulting in a higher likelihood of flash drought⁴⁰. Rewetting following a drought usually induced large, quick pulses in N_2O fluxes "hot moment"^{30,41,42}. A study found that hot moments lasted only a fourth of the study period, but could provide more than half of the N_2O fluxes in the soil⁴³. The major reason for a hot moment is drought-induced nitrogen substrate accumulation and their subsequent accessibility following rewetting⁴⁴. The response of hydroclimate processes to climatic differs across forests, leading to a latitudinal gradient of N_2O emissions. Our results confirm the above hypothesis, since MAP, Rin, and ET are the three largest relative contributors to N_2O emissions among many environmental factors (Fig. 6). Second, the texture of the soil can affect hydroclimate conditions and consequently N_2O emissions⁴⁵⁻⁴⁷. In general, soil texture influences N_2O emissions by determining the likelihood of anaerobic or aerobic soil conditions prevailing^{48,49}. Soil texture, for example, can influence water drainage during rainfall and drought, and hence the type of oxic and anoxic microsites of soil^{30,50}. N_2O emission was significantly enhanced in clayey soils, owing to its high water retention and low aeration, which favored to produce of anaerobic conditions, enhancing denitrification and rising N_2O fluxes^{51,52}. Soil clay decreases from tropical to boreal areas (Figure S8), which is a key factor contributing to the latitudinal gradient of N_2O emission. Third, rising temperatures in tropical areas may speed the decomposition of organic

materials in soils, providing energy and substrates to bacteria for denitrification and nitrification and therefore increasing N_2O emissions^{47,53}. Previous research has demonstrated that warming increases the rate of N cycling, resulting in an increase in soil N availability^{54,55}. Soil temperature is usually coupled with moisture in regulating N_2O emission, as higher temperatures can enhance microbial activity, while adequate soil moisture creates anaerobic conditions that promote denitrification⁵⁶. Therefore, the highest N_2O emissions occur in tropical forest zones under moist and warm conditions. Fourth, evapotranspiration (including evaporation and transpiration) decreases from tropical forests to boreal forests and can affect the latitudinal gradient of N_2O emissions. Studies have found that transpiration contributes to increasing N_2O by plant roots absorbing N_2O from soil water and releasing it into the atmosphere, thereby increasing N_2O in the surrounding soil^{15,57}. The transport of N_2O within the transpiration stream is a mechanism for emissions from tree stems and canopies. The similar latitude pattern between N_2O fluxes and evapotranspiration in this study supports this hypothesis.

There are two important implications of this study. One of them is that it can be used to validate the N_2O emission model results and provide key parameters for the simulation. Models are considered to be efficient research tools for calculating national and global N_2O emissions^{5,36,58}. However, there are large uncertainties in model calibration and validation, as well as sizable differences when simulating the spatial and temporal variations of N_2O emissions with various models^{59,60}. Overall, our results based on in situ field experiments validate the findings of some recent models¹⁹, showing N_2O emissions of tropical > temperate > boreal forests. To date, despite significant research efforts, accuracy in predicting N_2O generation and emission remains unsatisfactory, whether empirical or process-based models are used^{38,61}. Because models must account for a large range of complex regulatory characteristics when simulating worldwide N_2O emissions^{62,63}. Our research discovered that hydroclimate factors such as Rin, VPD, and ET are important in predicting forest N_2O emissions, and that incorporating these

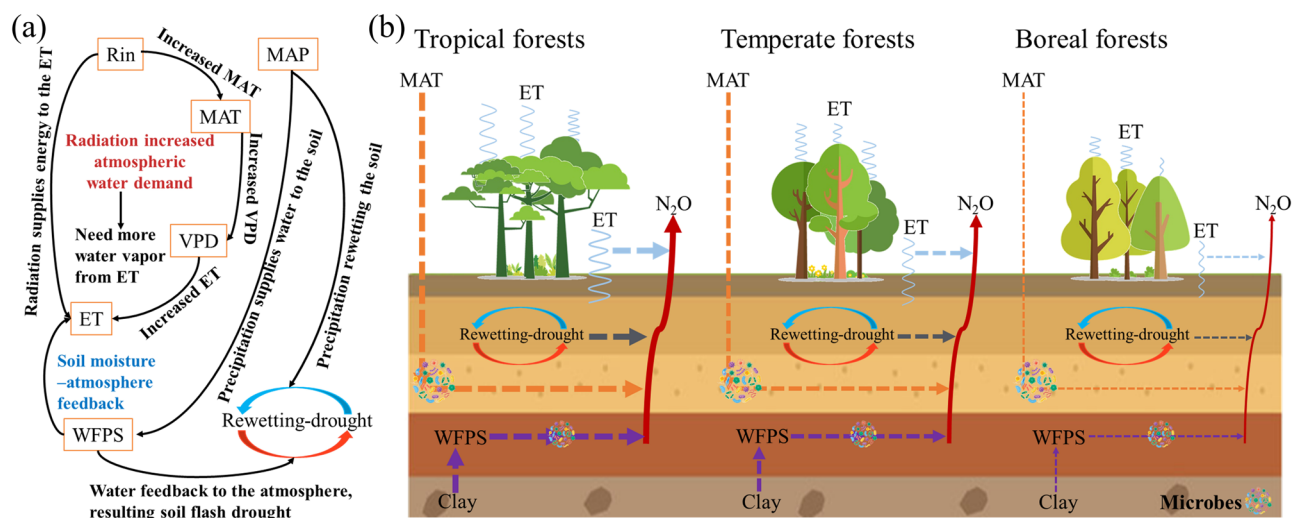


Fig. 8 | Conceptual diagram of how hydroclimate process influences N₂O fluxes. **a** Hydroclimate processes dominate soil drought and rewetting. **b** A comparative conceptual diagram of the four main potential mechanisms dominating N₂O flux emissions in different forests. The dashed arrows of different colors represent the pathways of influence of different factors on N₂O, the thicker the arrow, the greater the influence. Orange, purple, dark blue, and light blue represent the pathways of

temperature, clay, wet and dry alternation, and ET effect on N₂O flux, respectively. The red solid arrows represent N₂O fluxes. Rin incoming shortwave radiation, MAT mean annual temperature, VPD vapor pressure deficit, MAP annual precipitation, ET evapotranspiration, WFPS water-filled pore space. The background image was Created with BioRender.com (<https://biorender.com/>), and some elements were sourced from the Vecteezy database (<https://www.vecteezy.com/>).

components into the model may assist to enhance its accuracy. Another important implication is to enable new research horizons for N₂O field experiments. Over the past decades, many studies about the mechanisms regulating N₂O emissions have focused on soil factors^{64–66}. Currently, research on the influence of climate parameters on N₂O emissions focuses mostly on temperature and rainfall, which are insufficient to define the impact of climate, especially in the context of global climate change^{67,68}. And yet, despite our results indicating hydroclimate factors (e.g., Rin, ET, runoff, and VPD) potentially high contribution to global forests' N₂O emission, in situ studies of these factors on N₂O production are rare. In addition, the hydrological cycle's acceleration or intensification in response to global warming will be a persistent and challenging problem in climate study⁶⁹. Therefore, we suggest that it is time to expand our focus from land to the atmosphere and that it is now necessary to integrate N₂O emissions with more atmospheric factors, as the effects of atmospheric changes on soils will become increasingly evident.

Two uncertainties in this study are primarily caused by the data and methodology. The soil bacteria produce the majority of the world's N₂O during the N cycle^{35,70,71}. Denitrification and nitrification are the two key processes of soil N₂O production⁷². A recently global-scale study has been conducted that soil-moisture atmospheric feedback in hydroclimate processes plays an importance role in the balance between nitrifiers and denitrifiers¹⁶. However, the paucity of information on functional genes in this study creates uncertainty in the microbiological mechanisms by which hydrological cycles alter N₂O emissions. An in-depth understanding of climate change's effects on the coupling of soil characteristics, microbial populations, and N₂O emission pathways is critical for driving accurate biogeochemical models and identifying the dynamics of ecosystem N₂O emissions under climate change^{73,74}. To have a better mechanistic knowledge of the reactions of soil N₂O emissions to forest hydroclimate, more research should be conducted on the regulation of nitrifiers and denitrifiers. Forest types are classified according to latitude rather than biome, which creates uncertainty in this study. Moreover, plant species can influence soil microclimate and structure, N effectiveness, and root respiration, thus affecting N₂O emissions^{75–78}. For example, root secretions can stimulate denitrification activity and so increase N₂O generation in the soil⁴⁷. The response of different species to hydroclimate and their influence on it processes are different^{79–81}, which could affect soil N₂O emissions. For

instance, varying plant species canopies have varying effects on hydroclimate processes, which can ultimately affect soil N₂O emissions⁴³. Therefore, the mechanisms driving the changes in N₂O emissions by plant species at different latitudes need to be investigated further.

Our study finds for the first time that hydroclimate highly explains forest N₂O emissions at a global scale. We found that N₂O fluxes emissions significantly decreasing with latitudes, and the value of N₂O fluxes in tropical forests ($45.4 \pm 97.4 \mu\text{g}\cdot\text{m}^{-2}\cdot\text{h}^{-1}$) > temperate forests ($37.7 \pm 74.5 \mu\text{g}\cdot\text{m}^{-2}\cdot\text{h}^{-1}$) > boreal forests ($11.6 \pm 24.1 \mu\text{g}\cdot\text{m}^{-2}\cdot\text{h}^{-1}$). The hydroclimate factor contributed 78.2% of N₂O emissions, whereas the soil factor contributed 21.8%. Among the hydroclimate factors, MAP, ET, Rin, and runoff contributed the most to N₂O emissions. Our results provide new ideas for future field experiments, and we should improve the study of the effects of hydroclimate factors (such as evapotranspiration and solar radiation) on N₂O emissions. The key hydroclimate factors we found can be useful for N₂O models, and incorporating these dynamics may improve the prediction of global N₂O emissions. Overall, recognizing the primary causes of global forest N₂O emissions is critical for addressing the climate change dilemma.

Material and methods

Data collection

The N₂O emissions dataset was sampled from published articles. First, we searched Google Scholar (<https://scholar.google.com/>), Web of Science (<http://apps.webofknowledge.com>), and China National Knowledge Infrastructure Database (<http://www.cnki.net>) databases for publications containing the keywords “nitrous oxide” OR “N₂O” AND “forest”, “forestland”, “plant” OR “vegetation” up to December 30, 2022. Second, to ensure site comparability and mitigate selection bias, we applied the following criteria when extracting peer-reviewed publications: (a) inclusion of only field studies conducted in forest sites without anthropogenic N fertilization treatments; (b) location information of field experiments must be provided in the article; (c) consistent soil sampling from a standardized depth across all sites (between 0 ~ 20 cm); (d) standardization of units for each measured factor (e.g., N₂O fluxes emission standardized to $\mu\text{g N m}^{-2} \text{h}^{-1}$, cumulative N₂O emission standardized to kg N ha^{-1}); and (e) ensure that soil factors were measured as consistent method as possible across all sites, such as using oven drying method for SM and KCl extracts method for soil available N.

Table 1 | Summary of variables information

ID	Variables	Abbreviation	Data source
1	Latitude (°)	–	Published literature
2	Longitude (°)	–	Published literature
3	Altitude (m)	–	Published literature
4	Nitrous oxide emissions fluxes ($\mu\text{g N m}^{-2} \text{h}^{-1}$)	N ₂ O fluxes	Published literature
5	Cumulative Nitrous oxide emissions (kg N ha^{-1})	Cumulative N ₂ O	Published literature
6	Soil organic carbon (g kg^{-1})	SOC	Published literature
7	Soil total nitrogen (g kg^{-1})	Total N	Published literature
8	Soil organic carbon/total nitrogen	C/N	Published literature
9	Soil nitrate nitrogen (mg kg^{-1})	NO ₃ ⁻	Published literature
10	Soil ammonium nitrogen (mg kg^{-1})	NH ₄ ⁺	Published literature
11	Soil pH in the water	pH	Published literature
12	Bulk density (g cm^{-3})	BD	Published literature
13	Sand (%)	–	Published literature
14	Clay (%)	–	Published literature
15	Silt (%)	–	Published literature
16	Mean annual temperature (°C)	MAT	Published literature
17	Annual precipitation (mm year^{-1})	MAP	Published literature
18	Water-filled pore space (%)	WFPS	Published literature
19	Soil water content (%)	SM	Published literature
20	Aridity index	AI	CRU dataset
21	Mean annual incoming radiation (W m^{-2})	R _{in}	CRUNCEP dataset
22	Evapotranspiration (mm year^{-1})	ET	Zhang et al. ⁸⁵
23	Mean annual vapor pressure deficit (hPa)	VPD	ERA-Interim dataset
24	Annual runoff	Runoff	MAP minus ET

Soil factors: ID6 – 15; hydroclimate factors: ID16 – 24. CRUNCEP dataset: Climatic Research Unit of the National Centers for Environmental Prediction version 7 dataset; CRU dataset: Climatic Research Unit time-series dataset.

Finally, we compiled 272 observation samples of 69 study sites from 47 articles (references are listed in the supplementary information). These study sites cover a large forest area ($28^{\circ}15'46''\text{S}$ – $67^{\circ}26'26''\text{N}$ and $135^{\circ}13'48''\text{W}$ – $155^{\circ}14'23''\text{E}$) (Fig. 1), including tropical forests (25°S – 25°N , 22 sites, 61 observation samples), temperate forests (25°N – 50°N and 25°S – 50°S , 28 sites, 178 observation samples), and boreal forests (North of 50°N , 19 sites, 33 observation samples). Among the different forests, 31.9% of tropical forests, 40.6% of temperate forests, and 27.5% of boreal forests (Fig. 1).

Selection and description of characteristics

From all selected field studies, we collected N₂O fluxes or cumulative emissions data and the following parameters: coordinates (latitude and longitude), hydroclimate factors (MAT, MAP, SM, and WFPS), soil factors (clay, silt, and sand contents, pH, BD, TN, SOC, C/N, NH₄⁺, and NO₃⁻). Get Data Graph Digitizer (www.getdata-graph-digitizer.com/) was used to extract data from graphical plots.

Remote sensing and gridded data

We extracted multi-year mean AI, VPD, R_{in}, and ET from remote sensing and gridded data based on the coordinates of forest sites to investigate how hydroclimate affects N₂O emissions.

The water balance between the land surface and the atmosphere is represented by AI⁸². AI data were collected from the Climatic Research Unit time-series dataset (CRU TS3.21), which is derived from a wide network of weather station observations⁸³.

Land ET plays a crucial role in the water cycle and the soil moisture-atmosphere feedback loop in the climate system⁸⁴. ET was obtained from Zhang, et al.⁸⁵, which used a satellite remote sensing-based technique to calculate global terrestrial ET.

VPD is determined by the combination of atmospheric temperature and humidity, indicates atmospheric drought, and is used as a measure of atmospheric water demand⁸⁶. VPD was calculated from land air temperature and dew point temperature based on ERA-Interim dataset⁸⁷.

R_{in} represents energy availability and is important in dominating land surface temperature, VPD, and ET⁸⁸. R_{in} was obtained from Climatic Research Unit of the National Centers for Environmental Prediction dataset (CRUNCEP, version 7)⁸⁹.

Surface runoff is closely linked to precipitation and is a key part of the water cycle^{90,91}. In this work, runoff is calculated using the method of Lehner, et al.⁹² as precipitation minus evapotranspiration.

Data analysis

Nine hydroclimate factors and eleven soil factors were utilized to investigate the primary causes of N₂O emissions (Table 1). First, analysis of variance (ANOVA) was used to examine the changes in N₂O emissions (fluxes and cumulative emissions) and AI among various forests. Unless otherwise specified, $p < 0.05$ is often taken to signify statistically significant differences. Second, the correlation of each factor with latitude was analyzed by linear regression. The significance of linear regression analysis was calculated by the student's t-test. All statistical analyses were performed using SPSS 22.0 (Armonk, NY, USA), p values less than 0.05 indicate statistical significance (* $p < 0.05$, significant; ** $p < 0.01$, highly significant; and *** $p < 0.001$, extremely significant). Third, linear regression analysis was used to examine the relationship between N₂O fluxes and environmental factors. These factors have been determined to have significant latitudinal gradients in the second step of the analysis. Finally, we used the random forest to quantify each factor's relative importance in predicting the N₂O fluxes. Factors used for the random forest analysis were all those that proved to be significantly correlated

with N₂O fluxes by linear regression analysis in the third step. The random forest analysis was assessed with Python (version 3.7.3) package “sklearn”.

Data availability

Climatic research unit time-series dataset are available at <https://crudata.uea.ac.uk/cru/data/hrg/>. Climatic research unit of the national centers for environmental prediction dataset are available at <http://rda.ucar.edu/datasets/ds314.3/>. Land evapotranspiration data are available at http://files.ntsug.umt.edu/data/ET_global_monthly/. The ERA-Interim reanalysis dataset are available from the ECMWF (<https://www.ecmwf.int/>). N₂O emission and soil factor data used for this study are freely available from the corresponding author upon reasonable request.

Code availability

The SPSS and Python were used to both analyze the data and creating the figures. All relevant codes are available from the corresponding author upon reasonable request.

Received: 8 March 2024; Accepted: 7 August 2024;

Published online: 15 August 2024

References

- Feddema, J. J. et al. The importance of land-cover change in simulating future climates. *Science* **310**, 1674–1678 (2005).
- Grimm, N. B. et al. Global change and the ecology of cities. *Science* **319**, 756–760 (2008).
- Houghton, R. A. & Nassikas, A. A. Global and regional fluxes of carbon from land use and land cover change 1850–2015. *Glob. Biogeochem. Cycles* **31**, 456–472 (2017).
- Huang, H., Chen, D., Zhang, B., Zeng, L. & Dahlgren, R. A. Modeling and forecasting riverine dissolved inorganic nitrogen export using anthropogenic nitrogen inputs, hydroclimate, and land-use change. *J. Hydrol.* **517**, 95–104 (2014).
- Tian, H. et al. The global N₂O model intercomparison project. *Bull. Am. Meteorol. Soc.* **99**, 1231–1251 (2018).
- Bonan, G. B. Forests and climate change: forcings, feedbacks, and the climate benefits of forests. *Science* **320**, 1444–1449 (2008).
- FAO. *Global Forest Resources Assessment 2020—key Findings*. (2020).
- Bala, G. et al. Combined climate and carbon-cycle effects of large-scale deforestation. *Proc. Natl Acad. Sci. USA* **104**, 6550–6555 (2007).
- Luyssaert, S. et al. Old-growth forests as global carbon sinks. *Nature* **455**, 213–215 (2008).
- Pan, Y. et al. A large and persistent carbon sink in the world's forests. *Science* **333**, 988–993 (2011).
- Pugh, T. A. et al. Role of forest regrowth in global carbon sink dynamics. *Proc. Natl Acad. Sci. USA* **116**, 4382–4387 (2019).
- Green, J. K. & Keenan, T. F. The limits of forest carbon sequestration. *Science* **376**, 692–693 (2022).
- Ravishankara, A., Daniel, J. S. & Portmann, R. W. Nitrous oxide (N₂O): the dominant ozone-depleting substance emitted in the 21st century. *Science* **326**, 123–125 (2009).
- Ciais, P. et al. Climate change 2013: the physical science basis. *Contribution of Working Group I to the Fifth Assessment Report of the Intergovernmental Panel on Climate Change*. p. 465–570 (Cambridge University Press, 2014).
- Machacova, K., Vainio, E., Urban, O. & Pihlatie, M. Seasonal dynamics of stem N₂O exchange follow the physiological activity of boreal trees. *Nat. Commun.* **10**, 4989 (2019).
- Liao, J. et al. Soil moisture–atmosphere feedback dominates land N₂O nitrification emissions and denitrification reduction *Glob. Chang. Biol.* **28**, 6404–6418 (2022).
- Gundale, M. J. The impact of anthropogenic nitrogen deposition on global forests: negative impacts far exceed the carbon benefits. *Glob. Chang. Biol.* **28**, 690–692 (2022).
- Dalal, R. C. & Allen, D. E. Greenhouse gas fluxes from natural ecosystems. *Aust. J. Bot.* **56**, 369–407 (2008).
- Zhang, K. et al. Spatial and temporal variations of N₂O emissions from global forest and grassland ecosystems. *Agric. For. Meteorol.* **266**, 129–139 (2019).
- Tian, H. et al. A comprehensive quantification of global nitrous oxide sources and sinks. *Nature* **586**, 248–256 (2020).
- Zhu, Q., Schmidt, J. P., Buda, A. R., Bryant, R. B. & Folmar, G. J. Nitrogen loss from a mixed land use watershed as influenced by hydrology and seasons. *J. Hydrol.* **405**, 307–315 (2011).
- Ouyang, W., Xu, X., Hao, Z. & Gao, X. Effects of soil moisture content on upland nitrogen loss. *J. Hydrol.* **546**, 71–80 (2017).
- Kumar, R. et al. Strong hydroclimatic controls on vulnerability to subsurface nitrate contamination across Europe. *Nat. Commun.* **11**, 6302 (2020).
- Ehrhardt, S. et al. Nitrate transport and retention in Western European catchments are shaped by hydroclimate and subsurface properties. *Water Resour. Res.* **57**, e2020WR029469 (2021).
- Liu, W., Jiang, H., Zhang, J. & Xu, Z. Driving forces of nitrogen cycling and the climate feedback loops in the Yarlung Tsangpo River Basin, the highest-altitude large river basin in the world. *J. Hydrol.* **610**, 127974 (2022).
- Butterbach-Bahl, K., Baggs, E. M., Dannenmann, M., Kiese, R. & Zechmeister-Boltenstern, S. Nitrous oxide emissions from soils: how well do we understand the processes and their controls? *Philos. Trans. R. Soc. Lond. B Biol. Sci.* **368**, 20130122 (2013).
- Barrena, I. et al. Soil water content modulates the effect of the nitrification inhibitor 3, 4-dimethylpyrazole phosphate (DMPP) on nitrifying and denitrifying bacteria. *Geoderma* **303**, 1–8 (2017).
- Liao, J. et al. Biochar with large specific surface area recruits N₂O-reducing microbes and mitigate N₂O emission. *Soil Biol. Biochem.* **156**, 108212 (2021).
- Ledesma, J. L., Lupon, A., Martí, E. & Bernal, S. Hydrology and riparian forests drive carbon and nitrogen supply and DOC: NO₃⁻ stoichiometry along a headwater Mediterranean stream. *Hydrol. Earth. Syst. Sci.* **26**, 4209–4232 (2022).
- Harris, E. et al. Denitrifying pathways dominate nitrous oxide emissions from managed grassland during drought and rewetting. *Sci. Adv.* **7**, eabb7118 (2021).
- Gallarotti, N. et al. In-depth analysis of N₂O fluxes in tropical forest soils of the Congo Basin combining isotope and functional gene analysis. *ISME J.* **15**, 3357–3374 (2021).
- Xu, R. et al. Contrasting impacts of forests on cloud cover based on satellite observations. *Nat. Commun.* **13**, 670 (2022).
- Ryu, Y. et al. Atmospheric nitrous oxide variations on centennial time scales during the past two millennia. *Glob. Biogeochem. Cycles* **34**, e2020GB006568 (2020).
- Pasut, C., Tang, F. H., Hamilton, D., Riley, W. J. & Maggi, F. Spatiotemporal assessment of GHG emissions and nutrient sequestration linked to agronutrient runoff in global wetlands. *Glob. Biogeochem. Cycles* **35**, e2020GB006816 (2021).
- Smith, K. A. et al. Exchange of greenhouse gases between soil and atmosphere: interactions of soil physical factors and biological processes. *Eur. J. Soil Sci.* **54**, 779–791 (2003).
- Zhang, K. et al. Process-based TRIPLEX-GHG model for simulating N₂O emissions from global forests and grasslands: Model development and evaluation. *J. Adv. Model. Earth Syst.* **9**, 2079–2102 (2017).
- Groffman, P. M. et al. Challenges to incorporating spatially and temporally explicit phenomena (hotspots and hot moments) in denitrification models. *Biogeochemistry* **93**, 49–77 (2009).
- Kravchenko, A. et al. Hotspots of soil N₂O emission enhanced through water absorption by plant residue. *Nat. Geosci.* **10**, 496–500 (2017).
- Xu, S. et al. Linking N₂O emissions from biofertilizer-amended soil of tea plantations to the abundance and structure of N₂O-reducing microbial communities. *Environ. Sci. Technol.* **52**, 11338–11345 (2018).

40. Yuan, X. et al. A global transition to flash droughts under climate change. *Science* **380**, 187–191 (2023).
41. Zhou, Z. et al. Determining the hot spots and hot moments of soil N₂O emissions and mineral N leaching in a mixed landscape under subtropical monsoon climatic conditions. *Geoderma* **420**, 115896 (2022).
42. Zhang, K. et al. Moderate precipitation reduction enhances nitrogen cycling and soil nitrous oxide emissions in a semi-arid grassland. *Glob. Chang. Biol.* **29**, 3114–3129 (2023).
43. Mander, Ü. et al. Forest canopy mitigates soil N₂O emission during hot moments. *NPJ Clim. Atmos. Sci.* **4**, 39 (2021).
44. Barrat, H. A. et al. The impact of drought and rewetting on N₂O emissions from soil in temperate and Mediterranean climates. *Eur. J. Soil Sci.* **72**, 2504–2516 (2021).
45. Weitz, A. M., Linder, E., Frohling, S., Crill, P. & Keller, M. N₂O emissions from humid tropical agricultural soils: effects of soil moisture, texture and nitrogen availability. *Soil Biol. Biochem.* **33**, 1077–1093 (2001).
46. Laudone, G. et al. A model to predict the effects of soil structure on denitrification and N₂O emission. *J. Hydrol.* **409**, 283–290 (2011).
47. Wu, Y. F. et al. Diurnal variability in soil nitrous oxide emissions is a widespread phenomenon. *Glob. Change Biol.* **27**, 4950–4966 (2021).
48. Charles, A. et al. Global nitrous oxide emission factors from agricultural soils after addition of organic amendments: a meta-analysis. *Agric. Ecosyst. Environ.* **236**, 88–98 (2017).
49. Mei, K. et al. Stimulation of N₂O emission by conservation tillage management in agricultural lands: a meta-analysis. *Soil Tillage Res.* **182**, 86–93 (2018).
50. Leitner, S. et al. Linking NO and N₂O emission pulses with the mobilization of mineral and organic N upon rewetting dry soils. *Soil Biol. Biochem.* **115**, 461–466 (2017).
51. Skiba, U. & Ball, B. The effect of soil texture and soil drainage on emissions of nitric oxide and nitrous oxide. *Soil Use Manag.* **18**, 56–60 (2002).
52. Meurer, K. H. et al. Direct nitrous oxide (N₂O) fluxes from soils under different land use in Brazil—a critical review. *Environ. Res. Lett.* **11**, 023001 (2016).
53. Zhang, H., Zhou, G., Wang, Y., Tang, C. & Cai, Y. Clear-cut and forest regeneration increase soil N₂O emission in *Cunninghamia lanceolata* plantations. *Geoderma* **401**, 115238 (2021).
54. Yin, H., Chen, Z. & Liu, Q. Effects of experimental warming on soil N transformations of two coniferous species, Eastern Tibetan Plateau, China. *Soil Biol. Biochem.* **50**, 77–84 (2012).
55. Li, Y. et al. Effects of artificial warming on different soil organic carbon and nitrogen pools in a subtropical plantation. *Soil Biol. Biochem.* **124**, 161–167 (2018).
56. Luo, G., Kiese, R., Wolf, B. & Butterbach-Bahl, K. Effects of soil temperature and moisture on methane uptake and nitrous oxide emissions across three different ecosystem types. *Biogeosciences* **10**, 3205–3219 (2013).
57. Machacova, K., Papen, H., Kreuzwieser, J. & Rennenberg, H. Inundation strongly stimulates nitrous oxide emissions from stems of the upland tree *Fagus sylvatica* and the riparian tree *Alnus glutinosa*. *Plant Soil* **364**, 287–301 (2013).
58. Yao, Y. et al. Increased global nitrous oxide emissions from streams and rivers in the Anthropocene. *Nat. Clim. Change* **10**, 138–142 (2020).
59. Tian, H. et al. Global land-atmosphere exchange of methane and nitrous oxide: magnitude and spatiotemporal patterns. *Biogeosci. Discuss.* **10**, 19811–19865 (2013).
60. Zhang, J., Zhang, W., Jansson, P.-E. & Petersen, S. O. Modeling nitrous oxide emissions from agricultural soil incubation experiments using CoupModel. *Biogeosciences* **19**, 4811–4832 (2022).
61. Shcherbak, I., Millar, N. & Robertson, G. P. Global metaanalysis of the nonlinear response of soil nitrous oxide (N₂O) emissions to fertilizer nitrogen. *Proc. Natl Acad. Sci. USA* **111**, 9199–9204 (2014).
62. Saikawa, E., Schlosser, C. & Prinn, R. Global modeling of soil nitrous oxide emissions from natural processes. *Glob. Biogeochem. Cycles* **27**, 972–989 (2013).
63. Chen, H. et al. Modeling impacts of mulching and climate change on crop production and N₂O emission in the Loess Plateau of China. *Agric. For. Meteorol.* **268**, 86–97 (2019).
64. Dobbie, K. E. & Smith, K. A. Nitrous oxide emission factors for agricultural soils in Great Britain: the impact of soil water-filled pore space and other controlling variables. *Glob. Chang. Biol.* **9**, 204–218 (2003).
65. Li, Z. et al. Variations and controlling factors of soil denitrification rate. *Glob. Chang. Biol.* **28**, 2133–2145 (2022).
66. Lu, C. et al. Century-long changes and drivers of soil nitrous oxide (N₂O) emissions across the contiguous United States. *Glob. Chang. Biol.* **28**, 2505–2524 (2022).
67. Li, L. et al. Terrestrial N₂O emissions and related functional genes under climate change: a global meta-analysis. *Glob. Chang. Biol.* **26**, 931–943 (2020).
68. Heinzele, J. et al. Soil CH₄ and N₂O response diminishes during decadal soil warming in a temperate mountain forest. *Agric. For. Meteorol.* **329**, 109287 (2023).
69. Reid, A. J. et al. Emerging threats and persistent conservation challenges for freshwater biodiversity. *Biol. Rev.* **94**, 849–873 (2019).
70. Németh, D. D., Wagner-Riddle, C. & Dunfield, K. E. Abundance and gene expression in nitrifier and denitrifier communities associated with a field scale spring thaw N₂O flux event. *Soil Biol. Biochem.* **73**, 1–9 (2014).
71. Duan, P., Xiao, K., Jiang, Y. & Li, D. Mechanisms underlying the responses of soil N₂O production by ammonia oxidizers to nitrogen addition are mediated by topography in a subtropical forest. *Geoderma* **425**, 116036 (2022).
72. Wrage, N., Velthof, G. L., Van Beusichem, M. L. & Oenema, O. Role of nitrifier denitrification in the production of nitrous oxide. *Soil Biol. Biochem.* **33**, 1723–1732 (2001).
73. Tian, H. et al. Global soil nitrous oxide emissions since the preindustrial era estimated by an ensemble of terrestrial biosphere models: magnitude, attribution, and uncertainty. *Glob. Chang. Biol.* **25**, 640–659 (2019).
74. Wang, G., Huang, W., Zhou, G., Mayes, M. A. & Zhou, J. Modeling the processes of soil moisture in regulating microbial and carbon-nitrogen cycling. *J. Hydrol.* **585**, 124777 (2020).
75. Abalos, D., De Deyn, G. B., Kuyper, T. W. & Van Groenigen, J. W. Plant species identity surpasses species richness as a key driver of N₂O emissions from grassland. *Glob. Chang. Biol.* **20**, 265–275 (2014).
76. Benanti, G., Saunders, M., Tobin, B. & Osborne, B. Contrasting impacts of afforestation on nitrous oxide and methane emissions. *Agric. For. Meteorol.* **198**, 82–93 (2014).
77. Okiobe, S. T., Pirhofer-Walzl, K., Leifheit, E. F., Rillig, M. C. & Veresoglou, S. D. Proximal and distal mechanisms through which arbuscular mycorrhizal associations alter terrestrial denitrification. *Plant Soil* **476**, 315–336 (2022).
78. Hartmann, M. & Six, J. Soil structure and microbiome functions in agroecosystems. *Nat. Rev. Earth. Env* **4**, 4–18 (2023).
79. Elliott, K. J., Miniati, C. F., Pederson, N. & Laseter, S. H. Forest tree growth response to hydroclimate variability in the southern Appalachians. *Glob. Chang. Biol.* **21**, 4627–4641 (2015).
80. Powell, T. L. et al. Variation in hydroclimate sustains tropical forest biomass and promotes functional diversity. *New Phytol* **219**, 932–946 (2018).
81. Zhou, R., Wang, H., Duan, K. & Liu, B. Diverse responses of vegetation to hydroclimate across temporal scales in a humid subtropical region. *J. Hydrol. Reg. Stud.* **33**, 100775 (2021).
82. Schlaepfer, D. R. et al. Climate change reduces extent of temperate drylands and intensifies drought in deep soils. *Nat. Commun.* **8**, 14196 (2017).
83. Harris, I., Osborn, T. J., Jones, P. & Lister, D. Version 4 of the CRU TS monthly high-resolution gridded multivariate climate dataset. *Sci. Data* **7**, 109 (2020).

84. Jung, M. et al. Recent decline in the global land evapotranspiration trend due to limited moisture supply. *Nature* **467**, 951–954 (2010).
85. Zhang, K., Kimball, J. S., Nemani, R. R. & Running, S. W. A continuous satellite-derived global record of land surface evapotranspiration from 1983 to 2006. *Water Resour. Res.* **46**, 9 (2010).
86. Zhou, S., Zhang, Y., Park Williams, A. & Gentine, P. Projected increases in intensity, frequency, and terrestrial carbon costs of compound drought and aridity events. *Sci. Adv.* **5**, eaau5740 (2019).
87. Dee, D. P. et al. The ERA-Interim reanalysis: configuration and performance of the data assimilation system. *Quart. J. R. Meteorol. Soc.* **137**, 553–597 (2011).
88. Seneviratne, S. I. et al. Land radiative management as contributor to regional-scale climate adaptation and mitigation. *Nat. Geosci.* **11**, 88–96 (2018).
89. Viovy, N. *CRUNCEP Version 7-atmospheric Forcing Data For The Community Land Model.* (2018).
90. Dobrowski, S. Z. et al. The climate velocity of the contiguous United States during the 20th century. *Glob. Chang. Biol.* **19**, 241–251 (2013).
91. Miao, C. et al. The changing relationship between rainfall and surface runoff on the Loess Plateau, China. *J. Geophys. Res. Atmos.* **125**, e2019JD032053 (2020).
92. Lehner, F. et al. The potential to reduce uncertainty in regional runoff projections from climate models. *Nat. Clim. Change* **9**, 926–933 (2019).

Acknowledgements

We are grateful to the many researchers who assessed soil N₂O fluxes and other goal metrics. Their work is the foundation for the current data integration and global extrapolation. This study was financially supported by the National Natural Science Foundation of China (32201539), the Natural Science Foundation of Hunan Province (2024JJ5630), and Natural Science Foundation of Hunan Province (2022JJ40139).

Author contributions

In this study, S.L., and J.L. initiated and led the research. J.L. designed the investigation. J.L., S.L., and W.Z. extracted the data from literature and constructed the database. J.L. created the figures and wrote the paper.

All authors provided feedback and contributed to improving and finalizing the manuscript.

Competing interests

The authors declare no competing interests.

Additional information

Supplementary information The online version contains supplementary material available at <https://doi.org/10.1038/s41612-024-00737-8>.

Correspondence and requests for materials should be addressed to Sheng Lu.

Reprints and permissions information is available at <http://www.nature.com/reprints>

Publisher's note Springer Nature remains neutral with regard to jurisdictional claims in published maps and institutional affiliations.

Open Access This article is licensed under a Creative Commons Attribution-NonCommercial-NoDerivatives 4.0 International License, which permits any non-commercial use, sharing, distribution and reproduction in any medium or format, as long as you give appropriate credit to the original author(s) and the source, provide a link to the Creative Commons licence, and indicate if you modified the licensed material. You do not have permission under this licence to share adapted material derived from this article or parts of it. The images or other third party material in this article are included in the article's Creative Commons licence, unless indicated otherwise in a credit line to the material. If material is not included in the article's Creative Commons licence and your intended use is not permitted by statutory regulation or exceeds the permitted use, you will need to obtain permission directly from the copyright holder. To view a copy of this licence, visit <http://creativecommons.org/licenses/by-nc-nd/4.0/>.

© The Author(s) 2024